

Enhanced Supercapacitance with Porous Single-crystalline GaN Electrode^①

LI Hao^{a, b} XIE Kui^{b②}

^a(College of Chemical Engineering, Fuzhou University, Fuzhou 350116, China)

^b(Key Laboratory of Design and Assembly of Functional Nanostructures, Fujian Institute of Research on the Structure of Matter, Chinese Academy of Sciences, Fuzhou 350002, China)

ABSTRACT Capacitance is generally determined by the porous microstructure, electron conduction and the synergy effect of active sites in the porous electrode. In this work, we grew centimeter-scale metallic porous GaN single crystals with conductivity up to 18 S/cm at room temperature. The Cu-catecholates (Cu-CAT) nanowire arrays were grown on porous GaN single crystal to form porous single-crystalline electrode with enhanced supercapacitor performance. The Cu-CAT/GaN single crystalline electrode exhibits specific capacitance of 216 F/g and normalized capacitance of 40 $\mu\text{F}/\text{cm}^2$. After 5000 cycles, it retains 80% of its initial capacitance. The porous single-crystalline GaN electrode has high porosity and excellent conductivity showing high surface capacitance.

Keywords: supercapacitance, GaN single crystal, Cu-CAT nanowire arrays, single-crystalline electrode;

DOI: 10.14102/j.cnki.0254-5861.2011-3093

1 INTRODUCTION

Due to the fast charging and discharging process, and excellent cycling ability, supercapacitors (SCs) have great potential as an energy storage device^[1-4]. They are seen as candidates to fill the gap between batteries and traditional capacitors. Compared with traditional capacitors, the specific capacitance and energy density of SCs are increased by a factor of 100000 or even greater. By comparison with batteries, SCs can provide a faster charging and discharging rate over a time range of seconds or minutes. The SCs can charge and discharge 10 to 100 times as fast and cycle as the battery. However, the energy density is usually 3~30 times lower^[5, 6]. There is still an urgent need for new materials with high capacity to improve the energy density of SCs.

Gallium nitride single crystal is a semiconductor with wide and direct band gap, high carrier mobility and good stability^[7, 8]. Porous GaN single crystal was first demonstrated in situ inward epitaxial growth onto LiGaO₂ using chemical vapour deposition (CVD) by Xie and co-workers^[9]. Its electron concentration could be up to $3.3 \times$

10^{19} cm^{-3} and Hall mobility was as high as $30.4 \text{ cm}^2/(\text{V}\cdot\text{s})$, which suggested porous GaN has great potential in the field of electronics. Compared with bulk crystal, porous GaN single crystal has higher surface area. It provides more moving parts for making higher sensitivity sensors. Previous work showed that applying GaN as an SCs electrode could result in a good power density and cycling performance. But their specific capacitance needs to be further improved^[8, 10-13].

Metallic organic framework (MOFs) has aroused great interest because of its potential applications in supercapacitors due to its excellent porosity, high surface area and tunable pore sizes^[14-21]. Sheberla et al. first reported the high SCs performance of Ni₃(HITP)₂, a conductive MOF without any conductive additives or binders^[22]. Li et al. synthesized the Cu-CAT nanowire arrays (NWAs) and used them as electrode material for high performance SCs^[23]. When the current density was 0.5 A/g, the specific capacitance was about 120 F/g. The Cu-CAT nanowires with diameter between 200 to 250 nm were grown on carbon fiber paper. However, its length was at the micron level, which limited the improvement of performance.

Received 12 January 2021; accepted 5 March 2021

① This project was supported by the National Key Research and Development Program of China (2017YFA0700102), Natural Science Foundation of China (91845202), Dalian National Laboratory for Clean Energy (DNL180404) and Strategic Priority Research Program of Chinese Academy of Sciences (XDB2000000)

② Corresponding author. Xie Kui, Professor. Tel: +86-591-63179173. E-mail: kxie@fjirm.ac.cn

In this work, we prepared porous GaN single crystal at 1 cm scale by CVD methods, and its conductivity can reach 18 S/cm at room temperature. Then we grew Cu–CAT NWAs on the porous surface of a three-dimensional porous GaN single crystal to form crystalline NWAs on the nanometer scale in a controlled manner as the electrode material. By taking advantages of the high porosity nanostructure of Cu–CAT NWAs and excellent conductivity as well as porous GaN single crystal, it shows high areal capacitance and long cycling performance for SCs.

2 EXPERIMENTAL

2.1 Preparation of hierarchical structure

Cu–CAT NWAs on GaN single crystal

The porous GaN single crystal was grown on LiGaO₂ (001) substrates at 267 mbar and 950 °C in a flow rate of 200 sccm of NH₃ using CVD method. A solution of 24 mg (0.12 mmol) copper acetate monohydrate and 19.5 mg (0.06 mmol) 2,3,6,7,10,11-hexahydroxytriphenylene (HHTP) was distributed in 2400 μ L water and 600 μ L N,N-dimethylformamide (DMF) solvent. Subsequently, ultrasound dispersed evenly. The clean GaN single crystal was immersed into the mixture, reacted at 85 °C for 1~16 h in an oven and then cooled naturally. In order to activate Cu–CAT single crystals, GaN single crystal coated with Cu–CAT NWAs was immersed in deionized water and CH₃OH for 12 h respectively in a deionized vial at 85 °C, followed by drying in a vacuum at 85 °C for 12 h.

2.2 Performance testing of supercapacitors

SHIMADZU AUW 120D balance (D = 0.01 mg) with platform vibration isolator was used to weigh the mass of blank GaN single crystal carefully. After growth and activation, the Cu–CAT NWA coated GaN single crystal electrode was carefully weighed again, and the weight difference is the mass of Cu–CAT NWAs. The load mass of Cu–CAT NWAs was 0 to 0.60 mg/cm² by controlling the reaction time. The Cu–CAT NWAs on conductive porous GaN single crystal (mass loading 0.01, 0.03, 0.06, 0.10, 0.30 and 0.60 mg/cm²) by controlling the reaction time were used as the working electrode. The electrochemical measurements were made in a three-electrode system with a 3.0 M KCl aqueous electrolyte, using Hg/Hg₂SO₄ electrode as the reference electrode and Pt plate as the counter electrode. By changing the scanning range from 10 to 1000 mV/s and the current density between 0.5 to 10 A/g, CV curves and

constant current charge-discharge were measured within the potential range of 0~0.5 V relative to Hg/Hg₂SO₄. The specific capacitance is calculated based on the formula of $C = (I\Delta t)/(m\Delta V)$, where I (A), Δt (s), ΔV (V) and m (g) are the discharge current, discharge time, voltage range and the weight of the active material in working electrode correspondingly.

2.3 Characterization

The crystal phase of the samples was examined by X-ray diffraction (XRD) patterns (Rigaku MiniFlex II). The surface morphologies are analyzed by Field-emission scanning electron microscope (FE-SEM) (JEOL Ltd, Japan) with an accelerating voltage of 5 kV and transmission electron microscope (TEM) (FEI Ltd, USA) with an acceleration voltage of 200 kV. The TEM and 3D-reconstruction samples were both prepared by the FIB lift-out method. The conductivity tests were performed using DC four-terminal method (Keithley Instruments Inc., USA) and the oxygen partial pressure were changed by controlling the gas atmosphere. X-ray photoelectron spectroscopy (XPS) (Thermo, USA) was served to analyze the elemental valence states of the samples. The electrochemical characteristics were performed with electrochemical workstation (Zahner, Germany) at room temperature.

2.4 Theoretical methods

Vienna *Ab Initio* Simulation Package (VASP) code was used to perform density functional theory (DFT) calculations^[24]. Under the projector augmented wave (PAW) approach, the generalized gradient approach (GGA) was used including Perdew-Burke-Ernzerhof (PBE)^[25] functional to model the exchange correlation interactions. During the electron and geometric optimization, the energy and residual forces converge to 10⁻⁵ eV and 0.02 eV/Å, respectively.

The lattice parameters of the optimized LiGaO₂ crystal are $a = 5.50$, $b = 6.47$ and $c = 5.105$ Å with a 6×6×6 k -point grid. The cutoff energy was 520 eV. A $p(2\times 2)$ superstructure with four layers was used to simulate the periodic slab model for LiGaO₂(002) surface. The bottom two layers were fixed and the other atoms are relaxed. The vacuum region was 22 Å in thickness. A 3×3×1 k -point grid was used for these models for sampling in the Brillouin zone.

The energy for Cd defect is defined as:

$$E = E_{\text{defect}} - E_{\text{perfect}} + E_{\text{Li}}$$

Where E_{defect} is the energy of defect surface, E_{perfect} is the energy of perfect surface and E_{Li} is the energy of single Li atom.

The dopant formation energy for N atom according to the equation below:

$$E_{\text{for}} = E_{\text{N-doped}} - E_{\text{undoped}} + \mu_{\text{O}} - \mu_{\text{N}}$$

Where $E_{\text{N-doped}}$ and E_{undoped} are the energies of the KTaO_3 surface with and without nitrogen doping, μ_{O} and μ_{N} are the energies of O and N atoms taken from the energies of molecules O_2 and N_2 , respectively.^[26]

The optimized lattice parameters of GaN crystal are $a = b = 3.21 \text{ \AA}$, $c = 5.24 \text{ \AA}$, with an $8 \times 8 \times 6$ k -point grid. The plane-wave cutoff energy was 500 eV. A $p(2 \times 2)$ superstructure for GaN(0002) surface with four layers was used to simulate the periodic slab model. The bottom two layers were fixed and the other atoms are relaxed. A 22 \AA vacuum area was used to avoid interaction between the plate and its repeated images for these models. A $3 \times 3 \times 1$ k -point grid was used for these models for sampling in the Brillouin zone.

3 RESULTS AND DISCUSSION

3.1 Morphology and structural analysis of porous GaN single crystal

The crystalline structure of the as-synthesized GaN materials was investigated using XRD. As shown in Fig. 1a, the diffraction patterns show that the porous GaN single crystal is in the (0002) orientation. The digital photograph and the crystal structure could be seen in Fig. S2. Fig. 1b shows the SEM image of porous GaN single crystal, which

indicates that the pore structure has excellent three-dimensional connectivity. The hexagonal mesoporous structure uniformly covers the entire surface of the substrate. The average pore diameter is about 200 nm. To further analyze the internal structure of the pore structure, we carried out three-dimensional tomography of the porous single crystal and reconstructed the porous structure (Fig. 1c), which shows an excellent three-dimensional connectivity structure. The distribution curve of pore size is shown in Fig. 1d. The diameter of pore in the GaN single crystal is from 20 to 200 nm. The high resolution transmission electron microscope (HR-TEM) of the porous GaN single crystal is shown in Fig. 1e. It shows clearly ordered nitrogen and gallium atom array. The selected area electron diffraction (SAED) pattern shows a wurtzite GaN pattern without any other signs of intercalation or polycrystalline phenomena. The electrical conductivity of porous GaN single crystal at different temperature and oxygen partial pressure is depicted in Fig. 1f. The conductivity is about 18 S/cm at 25°C . The electric conductivity is high because there are many internal defects in the GaN porous single crystal. These defects lead to low resistance when the electric charge flows in the crystal. The increase in temperature or decrease in oxygen partial pressure will increase the conductivity. With good conductivity and porous structure, the GaN single crystal is suggested to be a potential electrode material for energy storage devices.

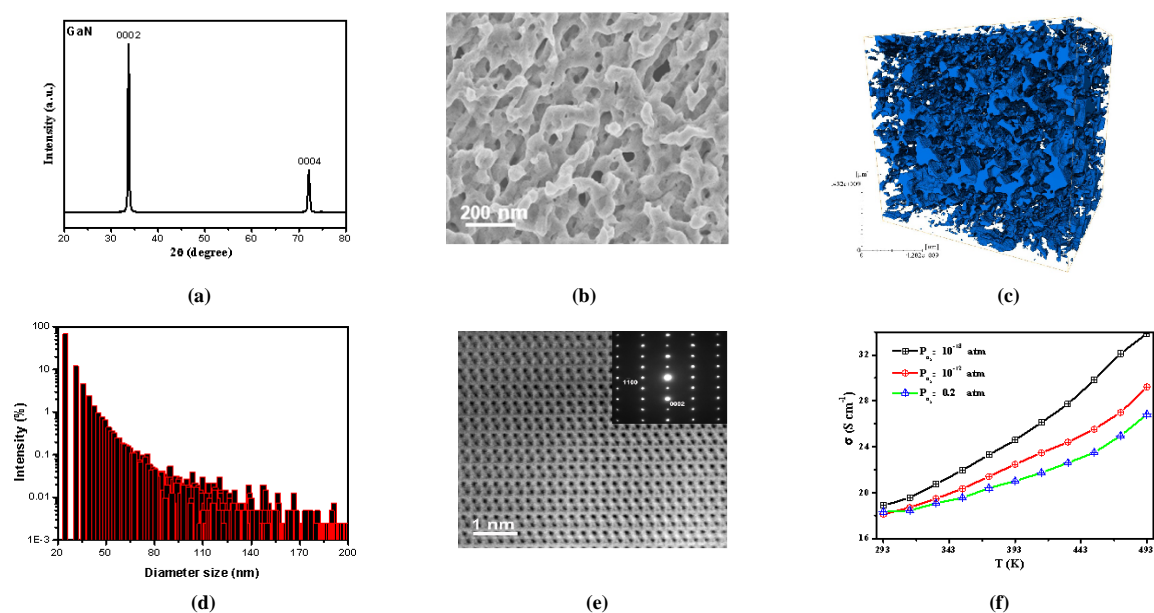


Fig. 1. (a) XRD pattern of porous GaN single crystal, (b) SEM image of the porous GaN single crystal with its exposed c -planes, (c) 3D model of all pores of porous GaN single crystal, (d) Discrete frequency of pore size of porous GaN single crystal, (e) Spherical aberration corrected scanning transmission electron microscope (Cs-corresponding STEM) image of porous GaN single crystal and SAED pattern (inset), (f) Electrical conductivity of porous GaN single crystal varying with temperature under different partial pressure of oxygen

We used density functional theory (DFT) calculation to better understand the conversion process of LiGaO_2 to GaN. The defect formation energy of Li defect and N dope on the (0002) orientation of LiGaO_2 were calculated. The defect configurations of LiGaO_2 (002) surface are shown in Figs. 2a~2c, and the optimized structure of GaN (0002) surface

in Fig. 2d. The calculated Li defect formation energy is 2.10 eV and the energy of N doping is 3.39 eV, which mean the process of Li deficiency is easier than N substitution. Thus, it can be speculated that Li loses first and then the N atom substitutes the O atom in the conversion progress of LiGaO_2 to GaN.

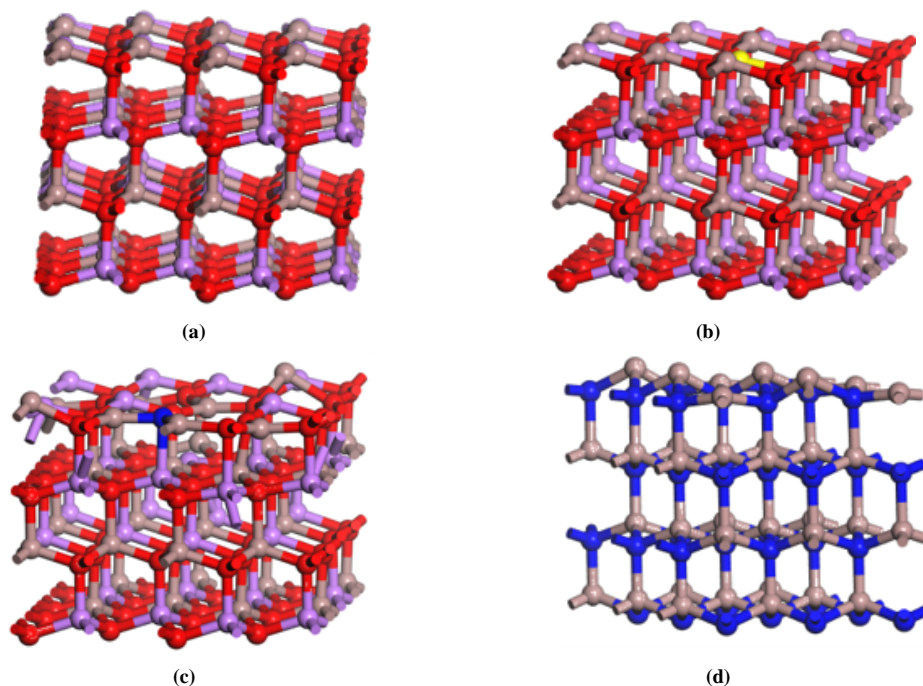


Fig. 2. (a~c) Different defect configurations of LiGaO_2 (002) surface, (a) Perfect surface, (b) Li atom defect, (c) N atom doped, (d) GaN (0002) surface (Li purple, N navy, O red, Ga brown)

3.2 Morphology and structural analysis of Cu-CATs

Cu-CAT NWAs were grown on porous GaN single crystal by immersing GaN single crystal into reaction solution, which is mixed by copper acetate monohydrate and HHTP in water/DMF solvent at 85 °C with the reaction time varying from 1 to 16 h. The XRD result shown in Fig. 3a indicates that Cu-CAT NWAs have grown on porous GaN single crystals without decreasing the crystallinity of gallium nitride. As depicted in Figs. S2a and S2b, the yellowish porous GaN single crystal is covered with Cu-CAT NWAs and turns dark blue. Fig. S2d shows the structure diagram of Cu-CAT NWAs. Figs. 3b~3d are the SEM images of Cu-CAT NWAs grown on porous GaN single crystal for 1, 6 and 12 h. The diameters of Cu-CAT NWAs are controlled between 10 to 50 nm, and the lengths are modulated between 10 and 200 nm to harvest higher specific surface area. The

survey XPS spectrum and energy dispersive X-ray spectroscopy (EDS) elemental mapping (Figs. S3 and S4) have detected the presence of Cu signals on the porous GaN single crystal, which proves that Cu-CAT NWAs have grown on porous GaN single crystal uniformly. The SEM image with higher magnification shown in Fig. 3e indicates the top facet of nanowires is uniform hexagonal. The TEM image is shown in Fig. 3f. The 1.83 nm distance between lattice fringes is consistent with the lattice spacing of [100] plane of Cu-CAT single crystal. According to the SEM and TEM results, the Cu-CAT nanowires have grown along the [001] direction. The 1D channel in Cu-CAT single crystal nanowires extends along the direction of growth. It can promote the transfer of electrolyte ions and realize the rapid charge transfer reaction, so as to obtain higher performance of SCs.

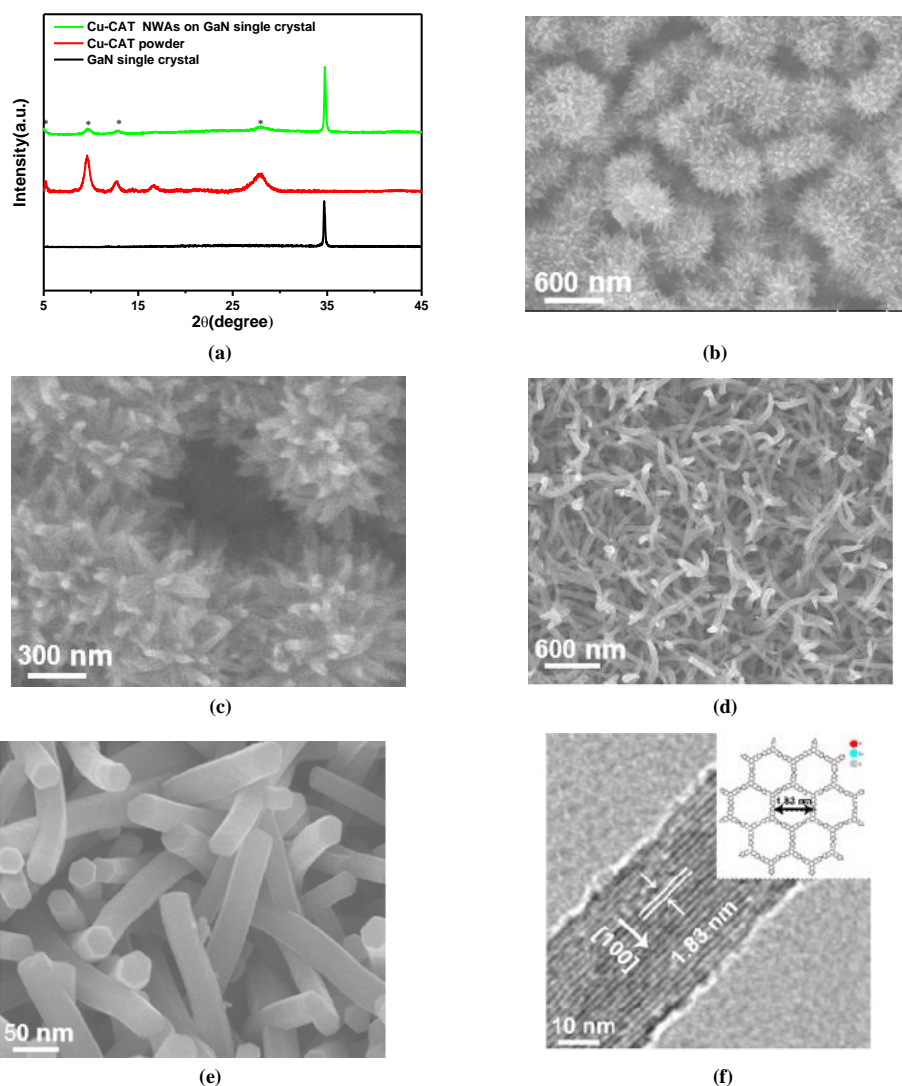


Fig. 3. (a) XRD patterns for Cu-CAT NWAs grown on porous GaN single crystal, (b~e) SEM images of the growth processes of Cu-CAT NWAs on porous GaN single crystal, (b), (c), (d) and (e) represent different reaction time of ~6, ~9 and ~12 h, (f) TEM image of Cu-CAT nanowires and crystal structure of Cu-CAT viewed along the *c*-axis (inset)

3.3 Supercapacitor performance

The electrochemical performances of hierarchical structure electrode in a three-electrode cell were characterized with Cu-CAT NWAs on porous GaN single crystal as the working electrode and 3 M KCl aqueous as the electrolyte. Fig. 4a shows the typical CV curves. The scan rate is between 20 and 1000 mV/s using Cu-CAT NWAs grown on porous GaN single crystal as the working electrode for 12 h. Fig. 4b shows the galvanostatic charge and discharge curves of Cu-CAT/GaN electrode. We explored the working potential window by cycling between 0 and 0.5 V (VS Hg/Hg₂SO₄). The CV curves in Fig. 4c show that the specific capacitance remains 55% when the scan rate increases 10 times from 10 to 100 mV/s, and retains 28% when the scan rate increases 100 times from 10 to 1000

mV/s. The cycle performance was tested at the scan rate of 500 mV/s (Fig. 4d). After 5,000 cycles, it keeps 80% of its original capacitance. Furthermore, the XRD pattern of the electrode does not change after cyclic test, which indicates that the electrode has excellent electrochemical stability. As shown in Fig. 4e, the specific current density varies as the reaction time and reaches the maximum of 436.8 A/g when the reaction time is 12 h. The Cu-CAT NWAs porous GaN single crystal electrode exhibits the specific capacitance of 216 F/g at 1.0 A/g. The specific surface area tested by Brunauer-Emmett-Teller (BET) method is 540 m²/g. The calculated normalized specific surface area capacitance is 40 μF/cm², which exceeds the values of other previously reported MOF-based SCs (Fig. 4f and Table S1), and is comparable to the graphene substrates.

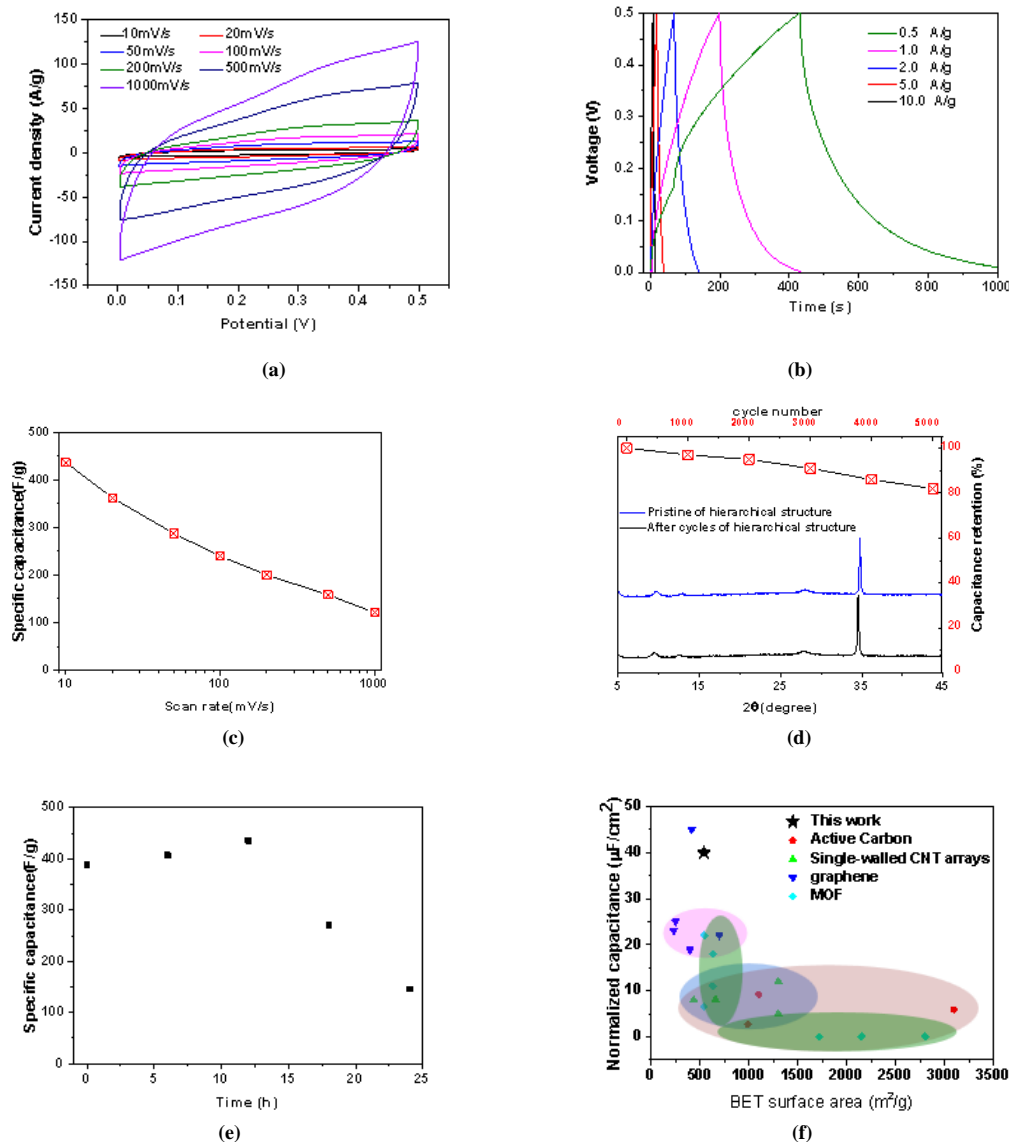


Fig. 4. (a)~(d) Electrochemical performances of Cu-CAT NWs/conductive porous GaN single crystal electrode in a three-electrode cell at 12h. (a) CVs at different scan rates. (b) Galvanostatic charge and discharge curves at different current densities. (c) Rate-dependent specific capacitance. (d) Cycling performance. (e) Electrochemical performances of Cu-CAT NWs/conductive porous GaN single crystal electrode in a three-electrode cell varying with different growing time. (f) Comparison of areal capacitances for various materials normalized relative to their BET surface areas

4 CONCLUSION

This work demonstrated the preparation of hierarchical single crystal structure materials and their applications in SCs. The conductive GaN single crystal with three-dimensional connected pore structure was grown on LiGaO₂ using CVD method. The Cu-CAT single crystal NWs were

grown on the porous GaN single crystal with controllable microstructure without any conductive additives or binders. The electrochemical performance of the porous single crystal GaN electrode reached 216 F/g at 1.0 A/g and showed a large normalized capacitance of 40 $\mu\text{F}/\text{cm}^2$. As an ideal electrode material of SCs, single crystal material with hierarchical structure has a broad development prospect.

REFERENCES

- (1) Wang, F. X.; Wu, X. W.; Yuan, X. H.; Liu, Z. C.; Zhang, Y.; Fu, L. J.; Zhu, Y. S.; Zhou, Q. M.; Wu, Y. P.; Huang, W. Latest advances in supercapacitors: from new electrode materials to novel device designs. *Chem. Soc. Rev.* **2017**, 46, 6816–6854.
- (2) Zhong, C.; Deng, Y. D.; Hu, W. B.; Qiao, J. L.; Zhang, L.; Zhang, J. J. A review of electrolyte materials and compositions for electrochemical

- supercapacitors. *Chem. Soc. Rev.* **2015**, 44, 7484–7539.
- (3) Yang, P. H.; Mai, W. J. Flexible solid-state electrochemical supercapacitors. *Nano Energy* **2014**, 8, 274–290.
- (4) Simon, P.; Gogotsi, Y. Materials for electrochemical capacitors. *Nat. Mater.* **2008**, 7, 845–854.
- (5) Shao, Y. L.; El-Kady, M. F.; Sun, J. Y.; Li, Y. G.; Zhang, Q. H.; Zhu, M. F.; Wang, H. Z.; Dunn, B.; Kaner, R. B. Design and mechanisms of asymmetric supercapacitors. *Chem. Rev.* **2018**, 118, 9233–9280.
- (6) González, A.; Goikolea, E.; Barrena, J. A.; Mysyk, R. Review on supercapacitors: technologies and materials. *Renew. Sust. Energ. Rev.* **2016**, 58, 1189–1206.
- (7) Kuykendall, T.; Pauzaskie, P.; Lee, S.; Zhang, Y. F.; Goldberger, J.; Yan, P. D. Metalorganic chemical vapor deposition route to GaN nanowires with triangular cross sections. *Nano Lett.* **2003**, 3, 1063–1066.
- (8) Yu, J. X.; Zhang, L.; Shen, J. X.; Xiu, Z. L.; Liu, S. W. Wafer-scale porous GaN single crystal substrates and their application in energy storage. *CrystEngComm*. **2016**, 18, 5149–5154.
- (9) Chen, C. L.; Sun, S. J.; Chou, M. M. C.; Xie, K. *In situ* inward epitaxial growth of bulk macroporous single crystals. *Nat. Commun.* **2017**, 8, 2178–8.
- (10) Zhang, L.; Wang, S. Z.; Shao, Y. L.; Wu, Y. Z.; Sun, C. L.; Huo, Q.; Zhang, B. G.; Hu, H. X.; Hao, X. P. One-step fabrication of porous GaN crystal membrane and its application in energy storage. *Sci. Rep.* **2017**, 7–9.
- (11) Wang, S. Z.; Shao, Y. L.; Liu, W. K.; Wu, Y. Z.; Hao, X. P. Elastic sandwich-type GaN/MnO₂/MnON composites for flexible supercapacitors with high energy density. *J. Mater. Chem. A* **2018**, 6, 13215–13224.
- (12) Wang, S. Z.; Zhang, L.; Sun, C. L.; Shao, Y. L.; Wu, Y. Z.; Lv, J. X.; Hao, X. P. Gallium nitride crystals: novel supercapacitor electrode materials. *Adv. Mater.* **2016**, 28, 3768–3776.
- (13) Wang, S. Z.; Sun, C. L.; Shao, Y. L.; Wu, Y. Z.; Zhang, L.; Hao, X. P. Self-supporting GaN nanowires/graphite paper: novel high-performance flexible supercapacitor electrodes. *Small* **2017**, 13, 1603330–9.
- (14) Shi, X. Y.; Yu, J. C.; Huang, J. L.; Chen, B.; Fang, L. J.; Shao, L. Y.; Sun, Z. P. Metal-organic framework derived high-content N, P and O-codoped Co/C composites as electrode materials for high performance supercapacitors. *J. Power Sources* **2020**, 467, 228304–9.
- (15) Shi, X. Y.; Yu, J. C.; Liu, Q. N.; Shao, L. Y.; Zhang, Y. Q.; Sun, Z. P.; Huang, H. T. Metal-organic-framework-derived N-, P-, and O-codoped nickel/carbon composites homogeneously decorated on reduced graphene oxide for energy storage. *ACS Appl. Nano Mater.* **2020**, 3, 5625–5636.
- (16) Liu, X. X.; Shi, C. D.; Zhai, C. W.; Cheng, M. L.; Liu, Q.; Wang, G. X. Cobalt-based layered metal-organic framework as an ultrahigh capacity supercapacitor electrode material. *ACS Appl. Mater. Inter.* **2016**, 8, 4585–4591.
- (17) Morozan, A.; Jaouen, F. Metal organic frameworks for electrochemical applications. *Energy Environ. Sci.* **2012**, 5, 9269–22.
- (18) Qu, C.; Jiao, Y.; Zhao, B. T.; Chen, D. C.; Zou, R. Q.; Walton, K. S.; Liu, M. L. Nickel-based pillared MOFs for high-performance supercapacitors: design, synthesis and stability study. *Nano Energy* **2016**, 26, 66–73.
- (19) Wang, L.; Han, Y. Z.; Feng, X.; Zhou, J. W.; Qi, P. F.; Wang, B. Metal-organic frameworks for energy storage: batteries and supercapacitors. *Coord. Chem. Rev.* **2016**, 307, 361–381.
- (20) Yang, J.; Zheng, C.; Xiong, P. X.; Li, Y. F.; Wei, M. D. Zn-doped Ni-MOF material with a high supercapacitive performance. *J. Mater. Chem. A* **2014**, 2, 19005–19010.
- (21) Zhang, X.; Qu, X.; Yang, S. X.; Fan, Q. Y.; Lei, D.; Liu, A.; Chen, X. Shape-controlled synthesis of Ni-based metal-organic frameworks with albizia flower-like spheres@nanosheets structure for high performance supercapacitors. *J. Colloid Interf. Sci.* **2020**, 575, 347–355.
- (22) Sheberla, D.; Bachman, J. C.; Elias, J. S.; Sun, C. J.; Horn, Y. S.; Dincă, M. Conductive MOF electrodes for stable supercapacitors with high areal capacitance. *Nat. Mater.* **2017**, 16, 220–225.
- (23) Li, W. H.; Ding, K.; Tian, H. R.; Yao, M. S.; Nath, B.; Deng, W. H.; Wang, Y. B.; Xu, G. Conductive metal-organic framework nanowire array electrodes for high-performance solid-state supercapacitors. *Adv. Funct. Mat.* **2017**, 27, 1702067–7.
- (24) Kresse, G.; Furthmüller, J. Efficiency of *ab-initio* total energy calculations for metals and semiconductors using a plane-wave basis set. *Comput. Mater. Sci.* **1996**, 6, 15–50.
- (25) Perdew, J. P.; Burke, K.; Ernzerhof, M. Generalized gradient approximation made simple. *Phys. Rev. Lett.* **1996**, 77, 3865–3868.
- (26) Modak, B.; Modak, P.; Ghosh, S. K. Improving visible light photocatalytic activity of NaNbO₃: a DFT based investigation. *RSC Adv.* **2016**, 6, 90188–90196.